Princeton Plasma Physics Laboratory

PPPL-4119
PPPL-4119

Gyrokinetic Stability Studies of the Microtearing Mode in the National Spherical Torus Experiment H-mode

J.A. Baumgaertel, M.H. Redi, R.V. Budny,
G. Rewoldt, and W. Dorland

October 2005

PRINCETON PLASMA PHYSICS LABORATORY

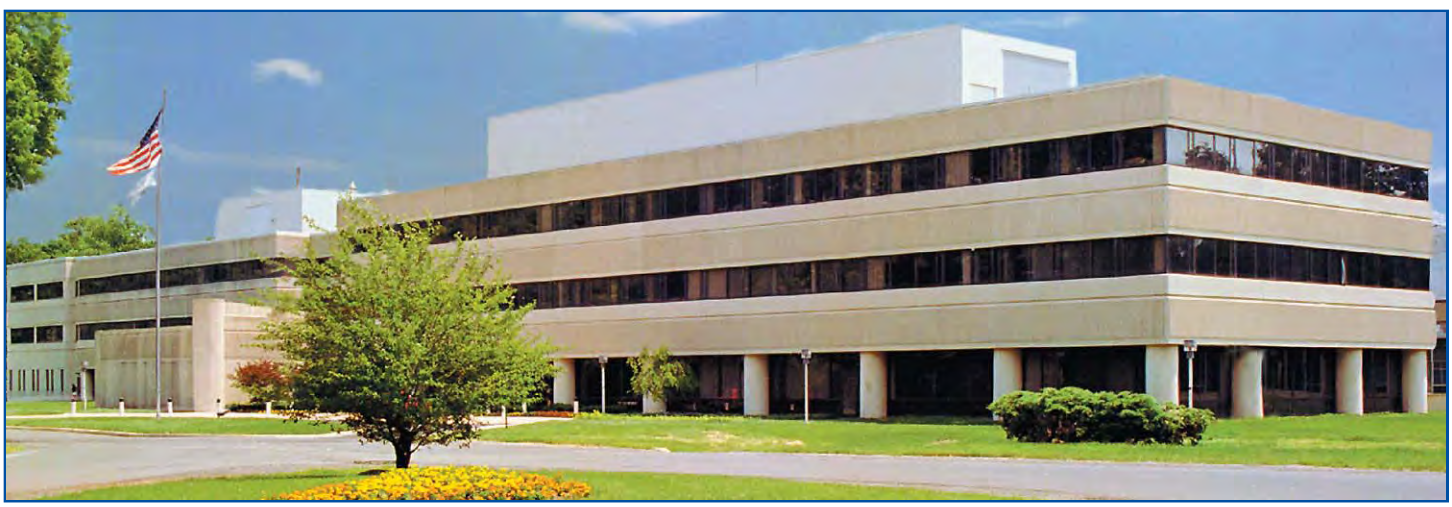

Prepared for the U.S. Department of Energy under Contract DE-AC02-76CH03073.

Gyrokinetic Stability Studies of the Microtearing Mode in the National Spherical Torus Experiment H-mode

Jessica Baumgaertel

Office of Science, Science Undergraduate Laboratory Internship (SULI)

University of Washington

Princeton Plasma Physics Laboratory

Princeton, NJ

August 19, 2005

Prepared in partial fulfillment of the requirements of the Office of Science, Department of Energy's Science Undergraduate Laboratory Internship under the direction of Dr. M. H. Redi at the Princeton Plasma Physics Laboratory.

Participant: ________________________________
Signature

Research Advisor: ________________________________
Signature

Table of Contents

Abstract

Gyrokinetic Stability Studies of the Microtearing Mode in the National Spherical Torus Experiment H-mode

J. A. BAUMGAERTEL (University of Washington, Seattle, WA, 98105)

M. H. REDI, R. V. BUDNY, G. REWOLDT (Princeton Plasma Physics Laboratory, Princeton, NJ, 08543) W. DORLAND (University of Maryland, College Park, MD 20742)

Insight into plasma microturbulence and transport is being sought using linear simulations of drift waves on the National Spherical Torus Experiment (NSTX), following a study of drift wave modes on the Alcator C-Mod Tokamak. Microturbulence is likely generated by instabilities of drift waves, which cause transport of heat and particles. Understanding this transport is important because the containment of heat and particles is required for the achievement of practical nuclear fusion. Microtearing modes may cause high heat transport through high electron thermal conductivity. It is hoped that microtearing will be stable along with good electron transport in the proposed low collisionality International Thermonuclear Experimental Reactor (ITER). Stability of the microtearing mode is investigated for conditions at mid-radius in a high density NSTX high performance (H-mode) plasma, which is compared to the proposed ITER plasmas. The microtearing mode is driven by the electron temperature gradient, and is believed to be mediated by ion collisions and magnetic shear. Calculations are based on input files produced by TRXPL following TRANSP (a time-dependent transport analysis code) analysis. The variability of unstable mode growth rates is examined as a function of ion and electron collisionalities using the parallel gyrokinetic computational code GS2. Results show the microtearing mode stability dependence for a range of plasma collisionalities. Computation verifies analytic predictions that higher collisionalities than in the NSTX experiment increase microtearing instability growth rates, but that the modes are stabilized at the highest values. There is a transition of the dominant mode in the collisionality scan to ion temperature gradient character at both high and low collisionalities. The calculations suggest that plasma electron thermal confinement may be greatly improved in the low-collisionality ITER.

I. Introduction

High anomalous plasma electron thermal conductivity, χ_e, and its associated heat transport has been a troubling problem in tokamak experiments for decades. The National Spherical Torus Experiment (NSTX) [1] exhibits extraordinarily good ion heat confinement and so provides an outstanding testbed to study electron thermal losses [2,3]. It is generally believed that the transport of plasma heat and particles is caused by microturbulence, which is likely generated by instabilities of drift waves. The containment of heat and particles is essential for the achievement of practical nuclear fusion. Therefore, it is an important consideration in the design of tokamaks, such as the proposed International Thermonuclear Experimental Reactor (ITER) [4-6]**.** Plasma microturbulence and transport is here investigated using linear gyrokinetic simulations of drift microtearing modes on NSTX. Implications for ITER thermal confinement will be drawn. Although H-mode NSTX densities and temperatures are much smaller than those planned for ITER, results from these simulations strongly support further computation of microtearing instabilities for ITER-like plasmas.

ITER is a high aspect ratio (A=R/a~3) tokamak, which will be built in Cadarache, France; completion expected in 2016. ITER will be a burning plasma experiment that is intended to provide sufficient insights into the physics and engineering required for a prototype fusion reactor.

A plasma drift wave is an oscillation of plasma particle densities and currents and their electrostatic and electromagnetic fields. They are caused by particle drifts due to the electric ($\vec{E}$) and magnetic ($\vec{B}$) fields in the tokamak plasma, such as the $\vec{E}\times\vec{B}$ drift of particles (Ref. [7], chapter 2). Charged particles move in a helical fashion around magnetic field lines, and in the presence of an electric field, they drift out of their helical orbits in a direction perpendicular to both $\vec{E}$ and $\vec{B}$. Drifts can also arise from curvature of magnetic field lines and magnetic field gradients.

Components of the microturbulent electrostatic and electromagnetic fields may be written as $\left\{S(k,\omega)e^{i(kx-\omega t)}\right\}$, each mode described by frequencies, ω, and wave vectors, $\vec{k}$. $k_\perp$ is perpendicular to the magnetic field line which wraps around a magnetic flux surface. The sign of ω denotes the direction gyration of the wave about the field line—the ion direction (positive ω) or electron (negative ω). Further details about drift wave physics may be found in reference [7], chapter 8.

The microtearing mode is a long wavelength, electromagnetic drift wave instability, with odd parity in the eigenfunctions of the electrostatic field. On NSTX gyrokinetic calculations find the normalized wave vectors in the range $0.1 < k_\perp \rho_s < 5.0$, where $\rho_s \equiv \frac{\sqrt{m_s T_e}}{eB}$ [8-10]. The microtearing mode creates small perturbations in the perpendicular magnetic field, pushing the field line towards the outside of the tokamak. The electrons follow the field lines, and carry their thermal energy with them away from the core, where high heat is necessary. Its longer wavelength MHD relative, the tearing mode, causes larger electromagnetic perturbations and can result in small magnetic islands.

Linear theory shows that the microtearing instability is driven by an electron temperature gradient, in the case of collisional plasma, and suppressed by magnetic shear. Analytic studies show that microtearing is mediated by collisionality and plasma resistivity. It is predicted that the microtearing mode is stable for high collision rates [7]. For moderate collision rates, the electron temperature gradient term dominates in the growth rate equation, driving the mode unstable [7]. However, for zero collisionality, analytic studies predict that the thermal force disappears and stabilizes the mode [7]. These predictions will be tested.

II. Materials and Methods

A. GS2 Input Preparation

To investigate the drift wave microturbulence as a function of collisionality, linear calculations of drift wave stability for data from NSTX shot 108730 [2, 8] were carried out using the massively parallel gyrokinetic code GS2 [11]. Figure 1 shows the time history of the shot and the time of interest at 0.4 seconds. The applied neutral beam power, plasma current, temperatures, D_α emission, and output heat profiles have reached a near steady state. The densities are still slowly increasing. Figure 2 depicts the radial profiles of the temperatures, electron density, and q for times 0.6 and 0.4 seconds. The calculations were carried out for a radius r/a of 0.65 and a time of 0.4 seconds.

The time dependent transport analysis code TRANSP [12] was used to analyze data from #108730 and TRXPL was used to create GS2 input files from the TRANSP output. These input files provide information such as specification of the plasma equilibrium configuration, the plasma location of interest, and parameters for each of the plasma species, including density, temperature, gradients of the density and temperature, and collisionalities (see Table I). An analytical Miller model equilibrium [13] is used, based on experimental data. The NSTX plasma was modeled with four species: electrons, deuterium, carbon impurities, and trace amounts of deuterium beam ions. The density at 0.65 is quite high, about $5.5\times10^{13}/cm^3$, while the temperatures are about 0.5KeV. Table I shows the input parameters of the base case. NSTX is a low-aspect ratio spherical torus; the modeled shot #108730 has aspect ratio, R/a=1.7.

In GS2, the collisionalities are calculated using a Lorentz collision model [14]. The Lorentz collision operator, $C(f_a)$, is also called the pitch-angle scattering operator, where $\xi = \upsilon_{\|}/\upsilon$ is the pitch angle. For electrons scattering off of electrons and slow ions:

(1) $$\frac{df_e}{dt} = C(f_e) = \nu_e(E)\frac{1}{2}\frac{\partial}{\partial\xi}\left[\left(1-\xi^2\right)\frac{\partial f_e}{\partial\xi}\right],$$

where f_e is a distribution function of electrons. It can be shown [8] that

(2) $$\nu_e(E) = \nu_{ei}\left(\frac{\upsilon_{2e}}{\upsilon}\right)^3\left[Z_{eff} + H_{ee}(\upsilon/\upsilon_{2e})\right],\text{ where } \upsilon_{2e} \equiv (2T_e/m_e)^{1/2}\text{, and}$$

(3) $$\nu_{ei} \equiv 4\pi n_e e^4 \log\lambda/[(2T_e)^{3/2} m_e^{\ 1/2}].$$

The electron collisionality input parameter for GS2 is

(4) $$\text{vnewk}_e = \nu_{ei} a\left(\frac{m_{ref}}{2T_{ref}}\right)^{1/2} = 0.002791\frac{n_{e19}\log\Lambda}{T_{e,keV}^{\ 3/2}}\frac{a_m A_{ref}^{\ 1/2}}{T_{ref,keV}^{\ 1/2}}.$$

The electron density, n_{e19}, is in units of $10^{19}/m^3$, normalizing scale a_m is in meters, and the normalizing reference species has temperature $T_{ref,keV}$ and atomic mass A_{ref}.

The ion-ion collisionality parameters are derived in terms of vnewk_e. Using an approximation that combines slow and fast ion collisions, the vnewk_i are given by

(5) $$\text{vnewk}_i = \text{vnewk}_e\left(\frac{m_e}{m_i}\right)^{1/2}\left(\frac{T_e}{T_i}\right)^{3/2} Z_i^{\ 2}\sum_j \frac{n_j Z_j^{\ 2}}{n_e}\frac{2}{1+(A_i/A_j)^{1/2}(T_j/T_i)^{1/2}},$$ where j sums over all species colliding with species *i*. See Ref. 15 for a detailed discussion of GS2 collisionalities.

B. Gyrokinetic Calculations

The perturbed distribution function of the plasma particles is given by the solution

$$f = f_0 + \left[e_j \phi \frac{\partial f_0}{\partial K} + g \exp\left(i \frac{\mathbf{v}_\perp \times \mathbf{b} \cdot \mathbf{k}_\perp}{\omega_{cj}} \right) \right], \qquad (6)$$

where $g(\mu, K, x)$ satisfies the gyrokinetic equation:

$$\frac{\partial g}{\partial t} + \mathrm{v}_\parallel \mathbf{b} \cdot \nabla g + i \mathbf{k}_\perp \cdot \mathbf{v}_g g = -\left[\omega \frac{\partial f_0}{\partial K} - \frac{\mathbf{b} \times \nabla f_0 \cdot \mathbf{k}_\perp}{\omega_{cj}} \right] \left[J_0(z) e_j (\phi - \mathrm{v}_\parallel A_\parallel) + \frac{2 J_1(z)}{z} \mu B_\parallel \right]. \qquad (7)$$

K is the kinetic energy of the particles, ϕ and $A_\parallel$ are perturbed potentials, $\mathbf{b} = \mathbf{B}/|\mathbf{B}|$, e_j is the charge of the particle *j*, $\omega_{cj} = e_j B / m_j$ is the cyclotron frequency of particle *j*, $J_0(z)$ and $J_1(z)$ are Bessel functions, $\mathrm{v}_\parallel$ and $\mathrm{v}_\perp$ are components of the particle velocity, $k_\perp$ is the perpendicular wave vector (inversely proportional to the wavelength of the drift wave), v_g is the guiding center velocity, and $z = k_\perp \mathrm{v}_\perp / \omega_{cj}$. (Reference [7], chapter 2.)

Computations were performed on the Department of Energy National Energy Research Scientific Computing Center's (NERSC) IBM 6000 SP, nicknamed Seaborg. Each simulation used four nodes, sixteen processors per node and took approximately 90 minutes to complete on the IBM SP.

The gyrokinetic calculations yield growth rates, γ, and real frequencies, ω, for each wave vector of the simulated drift wave. These values were examined for converged instability (positive γ and corresponding ω) after 10,000-50,000 timesteps in each case, and were plotted with EXCEL. The code GS2 also solves for the eigenfunctions of the electrostatic and the two components of the electromagnetic field for each wave vector. The ion temperature gradient (ITG) range of normalized wave vectors, 0.1 to 0.8, was chosen in order to model the longest wavelength microtearing instabilities, considered to be the most significant.

Hundreds of linear stability calculations were carried out, scaling specified input parameters for each case. In the ITG simulations run for Alcator C-Mod in reference [16], changes in parameters for new input files were tediously calculated by hand. The process was drastically improved with the construction of a utility script, written in PERL, to efficiently create input files with the desired modifications.

III. Results

The collisionality parameters for all species, ν_j, in GS2 were scaled by real factors, K_ν, such that $\nu_j = K_\nu \nu_j^{\exp}$, where $K_\nu \in [0, 10]$. The instability growth rates for each wave vector in the GS2 output files were examined for convergence after 5000-10,000 timesteps. Table II lists the maximum growth rates and real frequencies for each run. Maximum growth rates and corresponding real frequencies are plotted in Figure 3 for the scaling factor K_ν.

The sign of the real frequency and the parity of the electrostatic eigenfunction were used to identify the dominant drift wave mode at each growth rate. Negative real frequency and odd eigenfunction parity is characteristic of the microtearing mode, while a positive real frequency and even eigenfunction parity signifies the ITG mode. Figure 4 shows the evolution of the electrostatic eigenfunctions for the fastest growing mode as collisionality is increased from zero to ten.

IV. Discussion and Conclusion

Earlier work has shown [8] that the fastest growing drift wave mode at long wavelength (the ITG range) in this NSTX H-mode experiment changed for zero collisionality from microtearing to ITG. This computational result is reproduced in Figs. 3-4: the eigenfunctions have definite even parity when collisionalities are set to zero, and the real frequencies become positive. We have now found that the microtearing mode becomes subdominant to the ITG as collisionalities increase above K_v=4.

Analytic studies have predicted that the microtearing mode should disappear for low and high collisionality [7]. Our results support these conclusions. The growth rates in Figure 3 decrease as collisionality increases, the microtearing mode stabilizes and may become stable at higher collisionalities. As collisionality is lowered, the mode increases slowly before it is dominated by the ITG. The ITG growth rates peak around K_v=0.01 and then decrease at lower collisionalities. We wish to point out that at very high and low collisionality, K_v<0.3 and K_v>3, the calculations may not be accurate, as densities and temperatures should be self-consistent with collisionalities.

A recent decision to site the ITER burning plasma experiment motivates a comparison between this NSTX experiment and the ITER design parameters. We compare the NSTX parameters to three planned plasmas: ITER-FEAT and more recent modest ITER plan parameters are in Table III. The ITER aspect ratios are all near 3, higher than the NSTX H-mode case being studied.

Estimates to compare collisionalities of the ITER scenarios and the NSTX H-mode case can be made from ν_{ii} [4],

$$(8)\quad \nu_{ii}(0) \propto \left(\frac{n_i}{m_i^{1/2} T_i^{3/2}}\right)$$

Because NSTX uses deuterium plasmas and ITER uses a 50-50 deuterium-tritium mix, the ratio of masses will be 2/2.5. The three ITER scenarios (Table III) correspond to effective scaling factor K_ν~0.05, 0.03, and 0.02, using central density and temperature values for NSTX and ITER-FEAT and half radius values for the most recent ITER proposals.

These conclusions have important implications for ITER thermal confinement. Figure 3 suggests that in the low-collisionality ITER, the microtearing mode may be stable, leaving the ITG as the dominant drift wave instability. There are recent methods believed to be capable of controlling the ITG, which causes ion thermal transport [3]. ITG turbulence can be suppressed by sheared $\mathbf{E} \times \mathbf{B}$ flow [17], formation of transport barriers through negative magnetic shear [18] and control of such barriers [19]. Therefore, our study proposes that heat transport may be greatly reduced in ITER.

Future Work

It would be interesting to study the effects on the microtearing instability of changing plasma parameters to check the transition from NSTX to typical planned ITER plasma scenarios. A nonlinear check of the robustness of the linear simulations would be worthwhile, as would extensive nonlinear calculations to compare the electron thermal conductivity, χ_e, and heat flux to experiment to show whether or not the microtearing drift mode causes high χ_e. Studies of the effects of plasma resistivity and beta (ratio of plasma pressure to magnetic pressure) would be informative. Finally, questions remain about physics underlying some of the observations: Why does the ITG dominate below K_ν=0.25 and above K_ν=4? Why does the ITG growth rate decrease as collisionality approaches zero, and why does the eigenfunction become double peaked ITG above K_ν=4?

Acknowledgements

We would like to thank the U.S. Department of Energy and the Princeton Plasma Physics Laboratory for the opportunity to participate in the SULI program. We thank the NSTX experimental team for the data and analysis of the experiment and G. W. Hammett and D. R. Mikkelsen for discussion of gyrokinetics and collisionalities. We give special thanks to James Morgan for his dedicated efforts with the summer students, and to Justin Stimatze for his support of the technical aspects of this project. Work also supported by U. S. DOE Contract number DE-AC02-76CH03073.

References

[1] M. Ono, *et al.*, Nucl. Fusion **40**, 557 (2000).

[2] D. A. Gates, *et al.*, Phys. Plasmas, **10**, 1659 (2003).

[3] D. Stutman, *et al.*, "Studies of Improved Electron Confinement on NSTX", submitted to Nucl. Fus. (2004).

[4] ITER Physics Basis Editors, *et al.*, Nuc. Fusion **39**, 2137 (1999).

[5] D. J. Campbell, Phys. Plasmas **8**, 2041 (2003).

[6] R. V. Budny, Nuc. Fusion **42**, 1383 (2002). R. V. Budny, private communication (2005)

[7] J. A. Wesson, *Tokamaks,* Oxford University Press, New York, NY (1997).

[8] M. H. Redi, *et al.,* 30th European Physical Society Conference on Plasma Physics and Controlled Fusion, St. Petersburg, Russia, July, 2003, P-4.94.

[9] M. H. Redi, *et al.,* 31st European Physical Society Conference on Plasma Physics and Controlled Fusion, London,UK, June, 2004, P-2.162.

[10] M. H. Redi, *et al.,* to be published: 32nd European Physical Society Conference on Plasma Physics and Controlled Fusion, Taragona, Spain, June, 2005, P-5.041.

[11] M. Kotschenreuther, *et al*., Comp. Phys. Com. **88**, 128 (1995).

[12] R. J. Hawryluk, in *Physics of Plasmas Close to Thermonuclear Conditions*, edited by B. Coppi, G. G. Leotta, D. Pfirsch, R. Pozzoli, and E. Sindoni (Pergamon, Oxford, 1980), Vol. 1, p.19.

[13] R. L. Miller, *et al*., Phys. Plasmas**, 5**, 973 (1998).

[14] H. A. Lorentz, Arch. Néerl. **10**, 336 (1905).

[15] See GS2 website http://gs2.sourceforge.net, Collision Notes by G. W. Hammett.

[16] J. A. Baumgaertel, *et al*. DoE JUR (2005) in press.

[17] P. Terry, Rev. Mod. Phys. **72**, 109 (2000).

[18] X. Garbet, *et al*. , Plasma Phys. Control. Fusion **46**, B557 (2004).

[19] C. Challis, Plasma Phys. Control. Fusion **46**, B23 (2004).

[20] S. S. Medley, *et al*., "MHD-induced Energetic Ion Loss during H-mode Discharges in the National Spherical Torus Experiment (NSTX)", Princeton Plasma Physics Laboratory Report, PPPL-3931 (2004).

Table I. Plasma parameters of NSTX simulation at 0.4 seconds.

Parameter	r/a~0.65
q	2.54
$\hat{s}$	1.58
T_d/T_e	0.97
T_c/T_e	0.97
T_{Dbeam}/T_e	42
$-a_{ref}\nabla n_e/n_e$=$-a_{ref}\nabla n_c/n_c$	0.14
$-a_{ref}\nabla n_d/n_d$	0.09
$-a_{ref}\nabla n_{Dbeam}/n_{Dbeam}$	10.6
$-a_{ref}\nabla T_e/T_e$	3.08
$-a_{ref}\nabla T_d/T_d$=- $a_{ref}\nabla T_c/T_c$	4.47
$-a_{ref}\nabla T_{Dbeam}/T_{Dbeam}$	-0.64
ν_e/ν_d	22.99
ν_c/ν_d	9.71
ν_{Dbeam}/ν_d	0.0053
T_{ref}(keV)=T_e	0.46
a_{ref} (m)	0.66
$n_{ref}= n_e$ (m^{-3})	5.7x19
β_{ref}	0.05
Freq norm=$(T_{ref}/m_{ref})^{0.5}/a_{ref}$ (sec^{-1})	0.73

Table II. Wave vectors, growth rates and real frequencies of the fastest growing mode for each K_ν. The microtearing mode range dominant is shaded grey.

K_ν	Wave Vector	Growth Rate	Real Frequency
0	0.5	5.26	1.80
0.002	0.5	5.67	1.81
0.005	0.5	5.82	1.82
0.01	0.5	5.87	1.85
0.05	0.5	4.96	1.92
0.1	0.5	3.67	1.92
0.25	0.5	2.87	-2.57
0.5	0.5	2.79	-2.85
0.75	0.4	2.58	-2.51
1	0.4	2.36	-2.63
1.25	0.4	2.15	-2.74
1.5	0.4	1.93	-2.83
1.75	0.4	1.73	-2.92
2	0.4	1.54	-2.99
2.5	0.3	1.21	-2.40
3	0.4	0.88	-3.24
4	0.8	0.88	0.15
5	0.3	0.78	0.26
10	0.8	1.00	0.24

Table III. Comparison of parameters for NSTX case [2, 20] and three proposed ITER [4, 5, 6] scenarios.

Parameter	*NSTX*	*ITER [4]*	*ITER[6]*	*ITER[6]*
R(m)	1.0	8.1	6.4	6.5
a(m)	0.6	2.8	2.0	2.0
I_p(MA)	0.8	21	15	12
$B_T(0)$(T)	0.49	5.68	5.3	5.4
$N_e(0)(m^{-3})$	5×10^{19}	9.6×10^{19}	4×10^{19}	3.2×10^{19}
$T_i(0)$(keV)	1.5	15	12	17
Z_{eff}	2	1.9	1.5	2.3

Figures

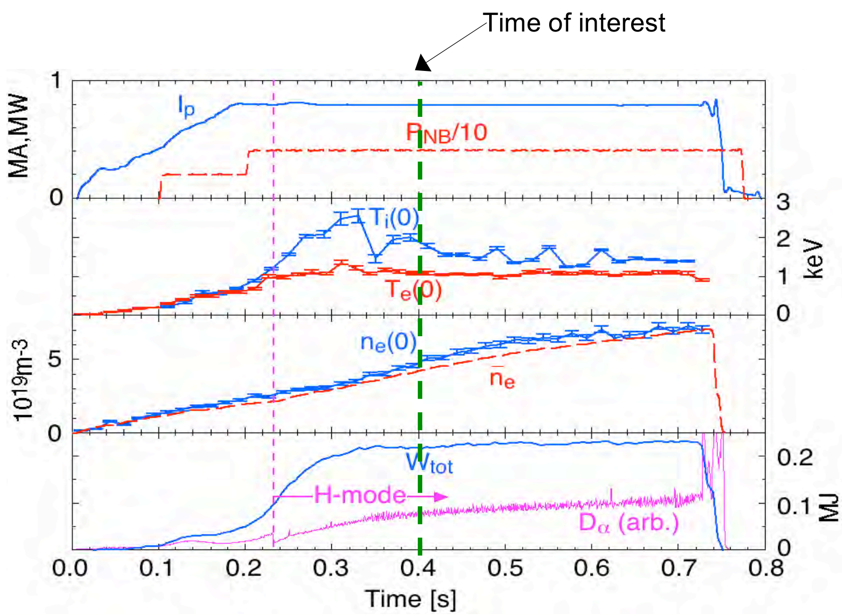

Figure 1. Time history of NSTX shot 108730; I_p is the plasma current, P_{NB} is the neutral beam power, $T_i(0)$ and $T_e(0)$ are the ion and electron temperatures at the center of the plasma, $n_e(0)$ is the electron density at the center of the plasma, $\bar{n}_e$ is the line averaged density, W_{tot} is the total stored energy, and D_α is the emission rate of D_α radiation.

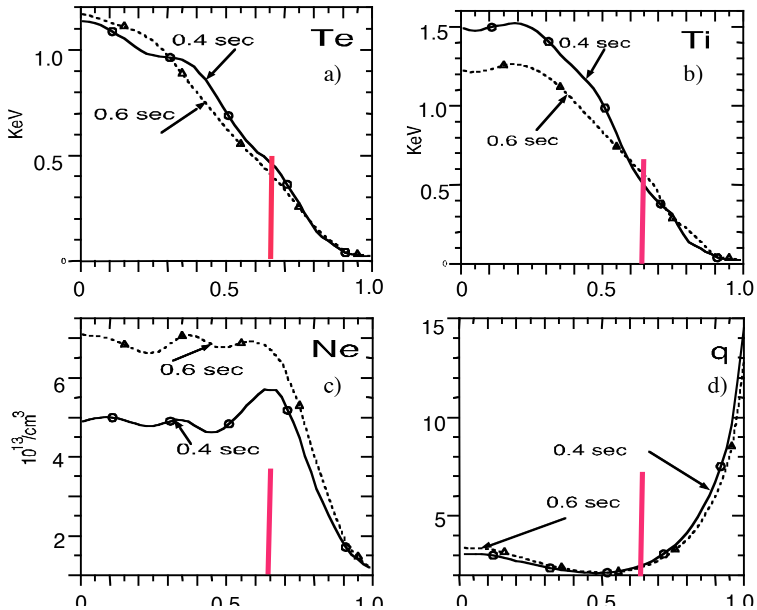

Figure 2. Temperature (a, b), density (c), and safety factor (d) profiles as a function of r/a in the plasma, at t=0.4 and 0.6 seconds. The time of interest is 0.4 seconds at the radius r/a=0.65 (red lines) for the calculation.

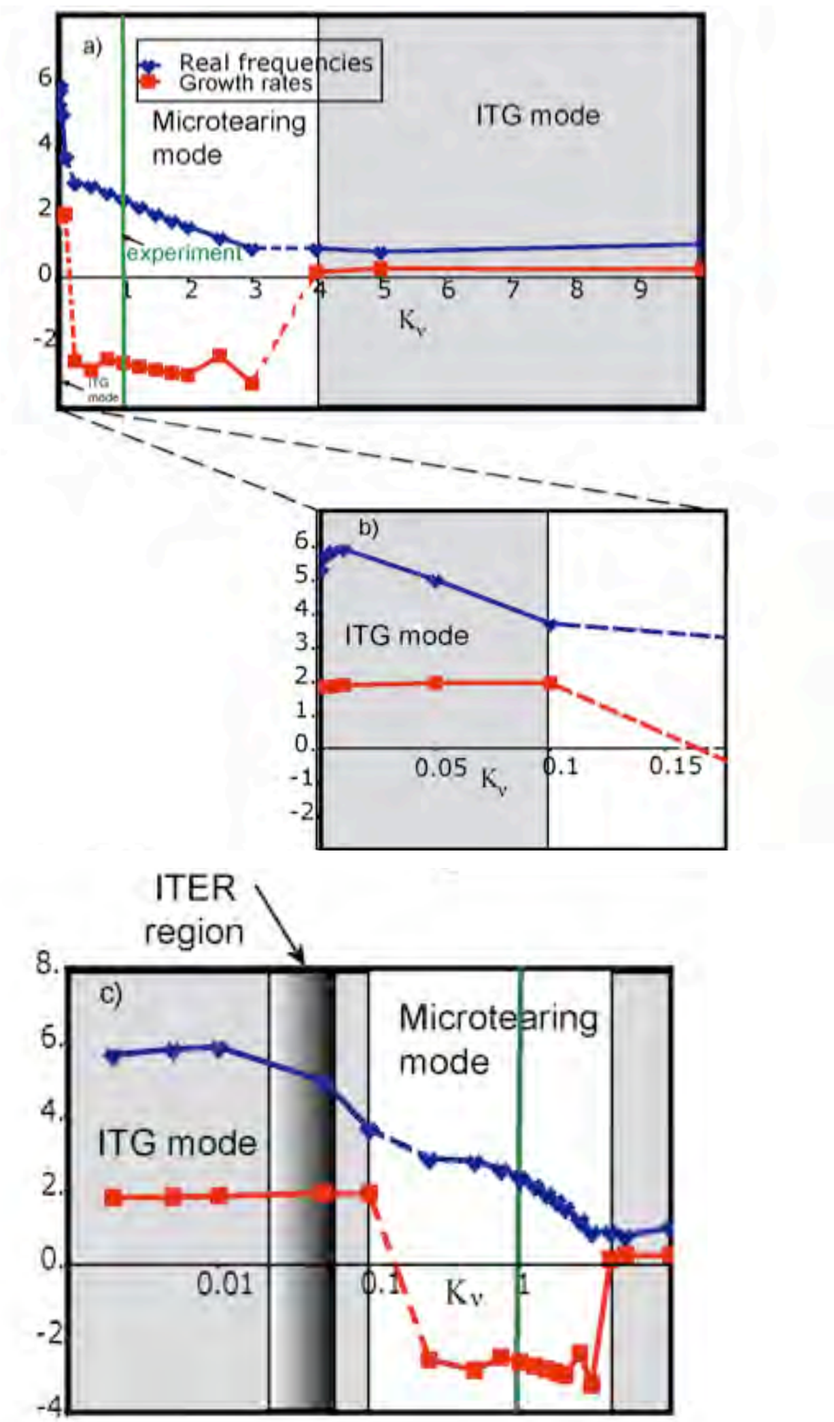

Figure 3. Growth rates and real frequencies (Mhz) of the fastest growing modes as a function of the collisionality scaling factor, K_ν, plotted on a linear scale (a, b) and log scale (c). The grey region indicates ITG mode, white indicates the microtearing mode, and the green line is the experimental value of the collisionality scaling factor, K_ν=1. The region of collisionalities for the proposed ITER plasmas is shown in (c).

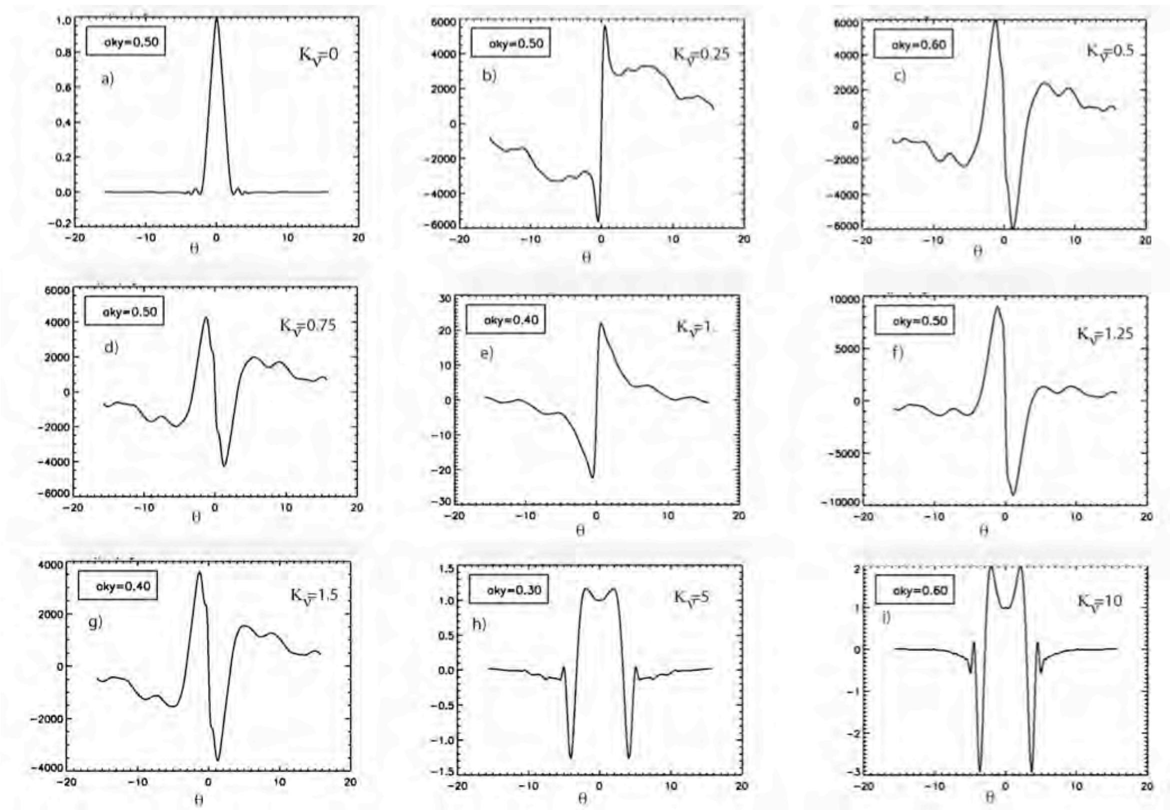

Figure 4. Evolution of electrostatic eigenfunctions for fastest growing mode as K_v increases from 0 to 10. The mode changes from single-peak ITG mode (a) to microtearing mode (b-g) to double-peaked ITG mode (h-i). θ is the poloidal field line angle.

External Distribution

Plasma Research Laboratory, Australian National University, Australia
Professor I.R. Jones, Flinders University, Australia
Professor João Canalle, Instituto de Fisica DEQ/IF - UERJ, Brazil
Mr. Gerson O. Ludwig, Instituto Nacional de Pesquisas, Brazil
Dr. P.H. Sakanaka, Instituto Fisica, Brazil
The Librarian, Culham Science Center, England
Mrs. S.A. Hutchinson, JET Library, England
Professor M.N. Bussac, Ecole Polytechnique, France
Librarian, Max-Planck-Institut für Plasmaphysik, Germany
Jolan Moldvai, Reports Library, Hungarian Academy of Sciences, Central Research Institute for Physics, Hungary
Dr. P. Kaw, Institute for Plasma Research, India
Ms. P.J. Pathak, Librarian, Institute for Plasma Research, India
Dr. Pandji Triadyaksa, Fakultas MIPA Universitas Diponegoro, Indonesia
Professor Sami Cuperman, Plasma Physics Group, Tel Aviv University, Israel
Ms. Clelia De Palo, Associazione EURATOM-ENEA, Italy
Dr. G. Grosso, Instituto di Fisica del Plasma, Italy
Librarian, Naka Fusion Research Establishment, JAERI, Japan
Library, Laboratory for Complex Energy Processes, Institute for Advanced Study, Kyoto University, Japan
Research Information Center, National Institute for Fusion Science, Japan
Professor Toshitaka Idehara, Director, Research Center for Development of Far-Infrared Region, Fukui University, Japan
Dr. O. Mitarai, Kyushu Tokai University, Japan
Mr. Adefila Olumide, Ilorin, Kwara State, Nigeria
Dr. Jiangang Li, Institute of Plasma Physics, Chinese Academy of Sciences, People's Republic of China
Professor Yuping Huo, School of Physical Science and Technology, People's Republic of China
Library, Academia Sinica, Institute of Plasma Physics, People's Republic of China
Librarian, Institute of Physics, Chinese Academy of Sciences, People's Republic of China
Dr. S. Mirnov, TRINITI, Troitsk, Russian Federation, Russia
Dr. V.S. Strelkov, Kurchatov Institute, Russian Federation, Russia
Kazi Firoz, UPJS, Kosice, Slovakia
Professor Peter Lukac, Katedra Fyziky Plazmy MFF UK, Mlynska dolina F-2, Komenskeho Univerzita, SK-842 15 Bratislava, Slovakia
Dr. G.S. Lee, Korea Basic Science Institute, South Korea
Dr. Rasulkhozha S. Sharafiddinov, Theoretical Physics Division, Insitute of Nuclear Physics, Uzbekistan
Institute for Plasma Research, University of Maryland, USA
Librarian, Fusion Energy Division, Oak Ridge National Laboratory, USA
Librarian, Institute of Fusion Studies, University of Texas, USA
Librarian, Magnetic Fusion Program, Lawrence Livermore National Laboratory, USA
Library, General Atomics, USA
Plasma Physics Group, Fusion Energy Research Program, University of California at San Diego, USA
Plasma Physics Library, Columbia University, USA
Alkesh Punjabi, Center for Fusion Research and Training, Hampton University, USA
Dr. W.M. Stacey, Fusion Research Center, Georgia Institute of Technology, USA
Director, Research Division, OFES, Washington, D.C. 20585-1290

The Princeton Plasma Physics Laboratory is operated
by Princeton University under contract
with the U.S. Department of Energy.

Information Services
Princeton Plasma Physics Laboratory
P.O. Box 451
Princeton, NJ 08543

Phone: 609-243-2750
Fax: 609-243-2751
e-mail: pppl_info@pppl.gov
Internet Address: http://www.pppl.gov